Mapping phytoplankton fluorescence properties with hyperspectral EnMAP data

Peter Gege*[1], Krista Alikas[2], Kersti Kangro[2], Nicole Pinnel[1], Stefan Plattner[1], Ian Somlai-Schweiger[1], Mirjam Uusõue[2]

[1]Deutsches Zentrum für Luft- und Raumfahrt (DLR), Remote Sensing Technology Institute, Oberpfaffenhofen, 82234 Wessling, Germany
[2]Tartu Observatory, Tartu University, Tõravere, Observatooriumi 1, 61602, Estonia
*Corresponding author: peter.gege@dlr.de

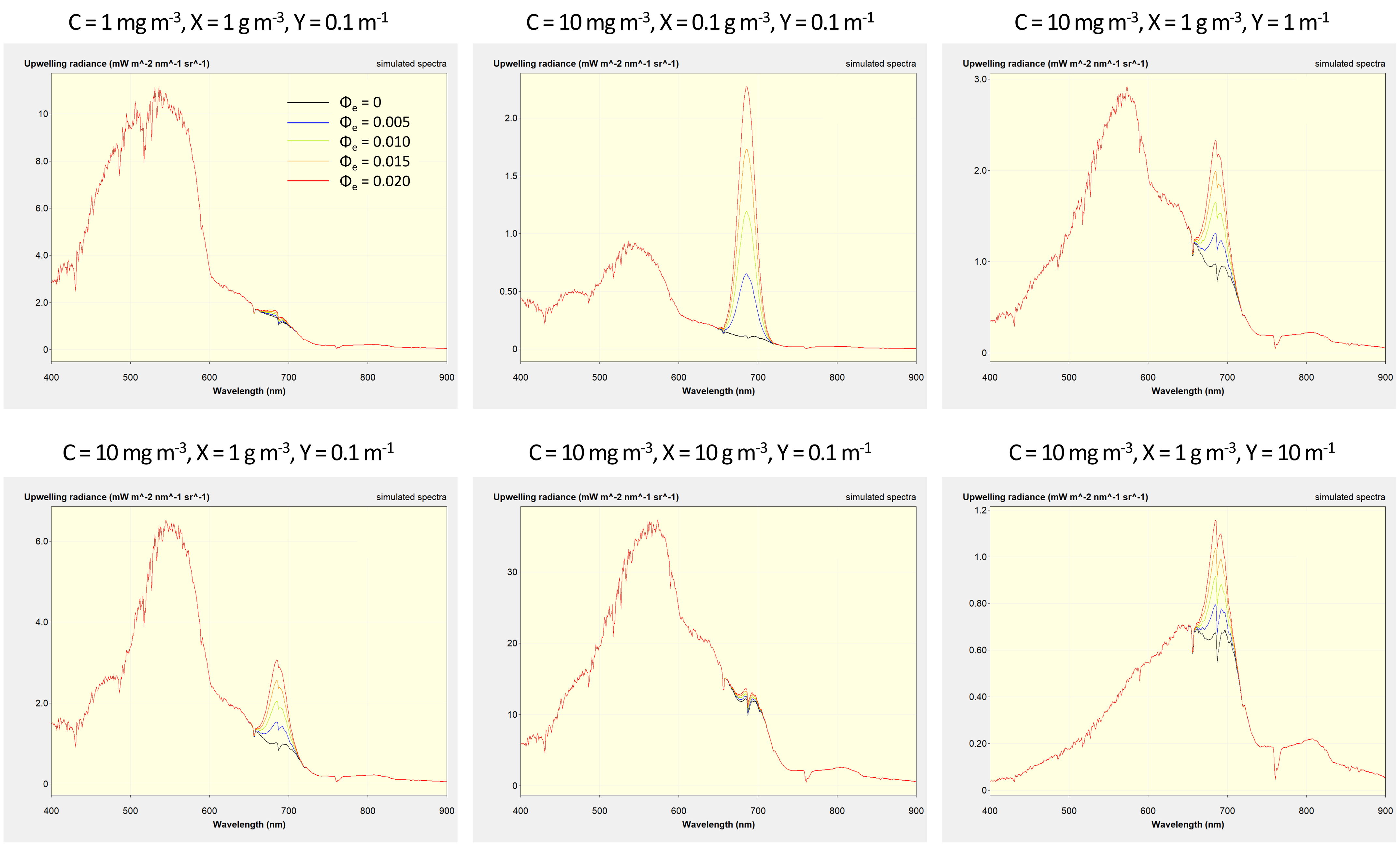

Fig. 1: Illustration of the dependency of water leaving radiance on phytoplankton concentration (C), total suspended matter concentration (X), CDOM absorption at 440 nm (Y) and fluorescence quantum efficiency (Φ_e). The simulations were made with WASI for green algae, an emission wavelength of 685 nm and a sun zenith angle of 40°.

Phytoplankton fluorescence

Phytoplankton exhibits a characteristic fluorescence peak near 685 nm with a FWHM of 25 nm. At high intracellular chlorophyll concentration, the emission wavelength (λ_e) may shift toward longer wavelengths due to reabsorption within the cells. The fluorescence quantum yield (Φ), defined as the ratio of emitted to absorbed photons within the 400–700 nm spectral range, quantifies the efficiency of photosynthesis and serves as a key indicator of light stress and nutrient limitation in primary production.

Model

The upwelling spectral radiance from a homogeneous water layer extending from depth z to z_B caused by phytoplankton fluorescence is given by[(1)]:

$$L_F(\lambda, z) = \frac{\Phi(\lambda)}{4\pi\lambda}\int_{PAR}\sum_i C_i\, a_i^*(\lambda')\left[e^{-K(\lambda')\cdot z} - e^{-K(\lambda')\cdot z_B - k_u(\lambda)\cdot(z_B - z)}\right]\frac{E_0(\lambda', 0)}{K(\lambda') + k_u(\lambda)}\lambda' d\lambda'$$

$\Phi(\lambda)$ denotes the fluorescence quantum yield at wavelength λ, C_i the concentration of phytoplankton group i, $a_i^*(\lambda)$ its specific absorption coefficient, $K(\lambda)$ the attenuation coefficient of downwelling irradiance, $k_u(\lambda)$ the attenuation coefficient of upwelling radiance, and $E_0(\lambda, 0)$ the downwelling vector irradiance just below the water surface. $\Phi(\lambda)$ is modelled with a Gaussian function centered at wavelength λ_e and a standard deviation of 10.6 nm. PAR is the photosynthetically active range from 400 to 700 nm.

$K(\lambda)$ and $k_u(\lambda)$ are parameterized in terms of the absorption coefficient $a(\lambda)$ and the backscattering coefficient $b_b(\lambda)$ of the water layer, expressed in terms of absorption by pure water, phytoplankton and CDOM, and backscattering by pure water and total suspended matter. Fig. 1 illustrates the dependency of water leaving radiance, i.e. $L_F(\lambda, 0)$ plus radiance backscattered in water, at the water surface (z = 0) for optically deep water ($z_B = \infty$) on the concentrations of the three major groups of water constituents.

Fluorescence retrieval

The described model is implemented in WASI[(2)] for forward simulation and AI-enhanced inverse modeling in optically deep and shallow water. Fig. 2 and Fig. 3 show results for EnMAP data from a coastal area and a lake. Besides the presented results for C, $\Phi_e = \Phi(\lambda_e)$ and λ_e, also sun glint, TSM concentration and CDOM absorption at 440 nm were derived. The uncertainty (R^2, RMSE) caused by spectral ambiguities ("overfitting") was determined by comparing the results of physical inversion and AI for 128 randomly chosen water pixels.

The two examples demonstrate the capability to map Φ_e and λ_e, alongside phytoplankton concentration C, using hyperspectral EnMAP data under conditions of high C. We applied the approach also to EnMAP images with low C, but didn't get consistent results for Φ_e and λ_e if the peak was not clearly visible in the data.

(1) See WASI handbook for a derivation of the equation
(2) WASI including documentation can be downloaded from https://ioccg.org/software

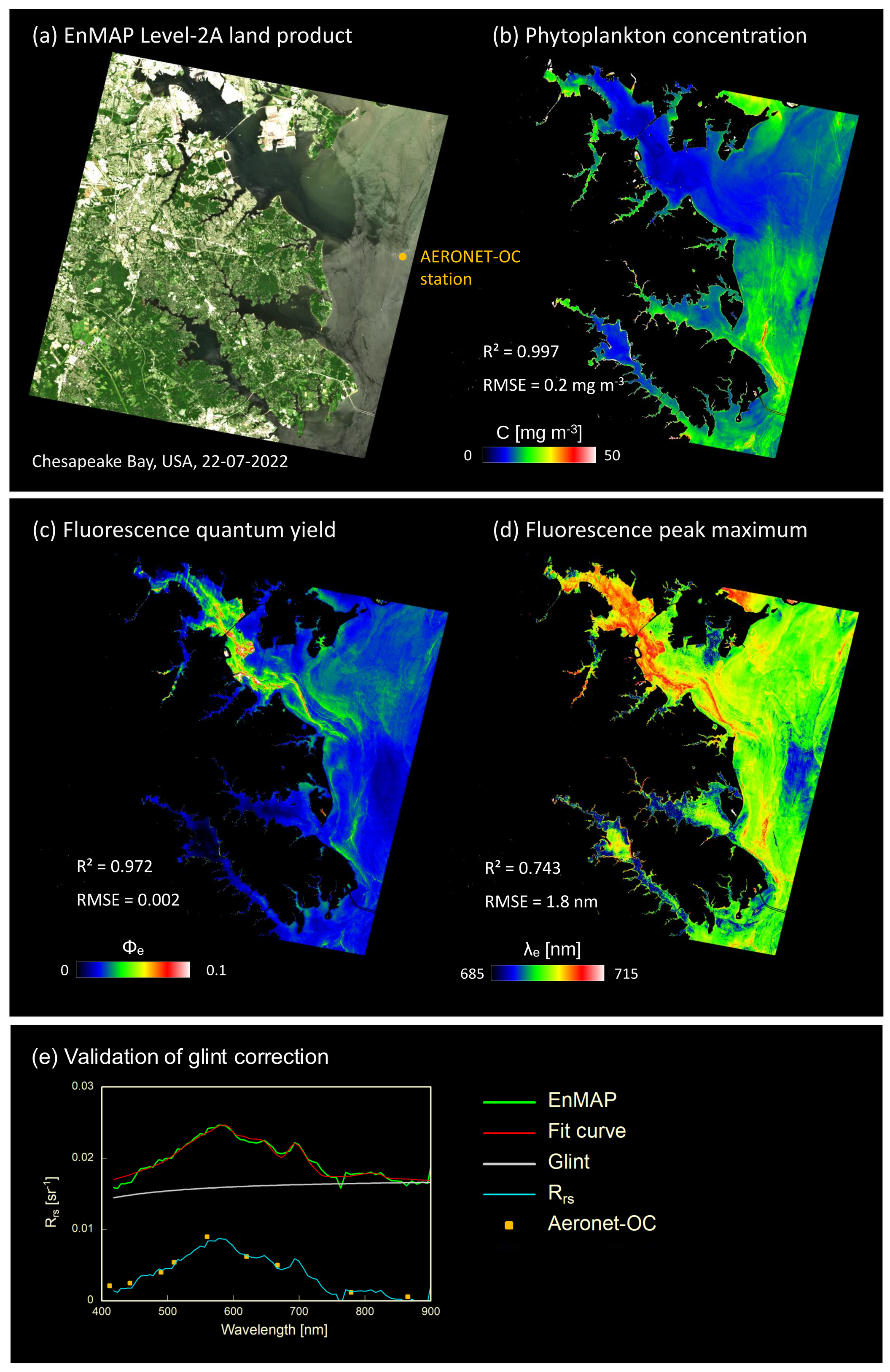

Fig. 2: Results for Chesapeake Bay, USA. (a) EnMAP image. (b) Phytoplankton concentration map. Dinoflagellates were determined as the dominating group. (c) Quantum yield map. (d) Peak maximum map. (e) Validation of glint correction. Sun glint is very high in large parts of the image, including the AERONET-OC site providing validation data. The plot shows that the glint correction procedure works well.

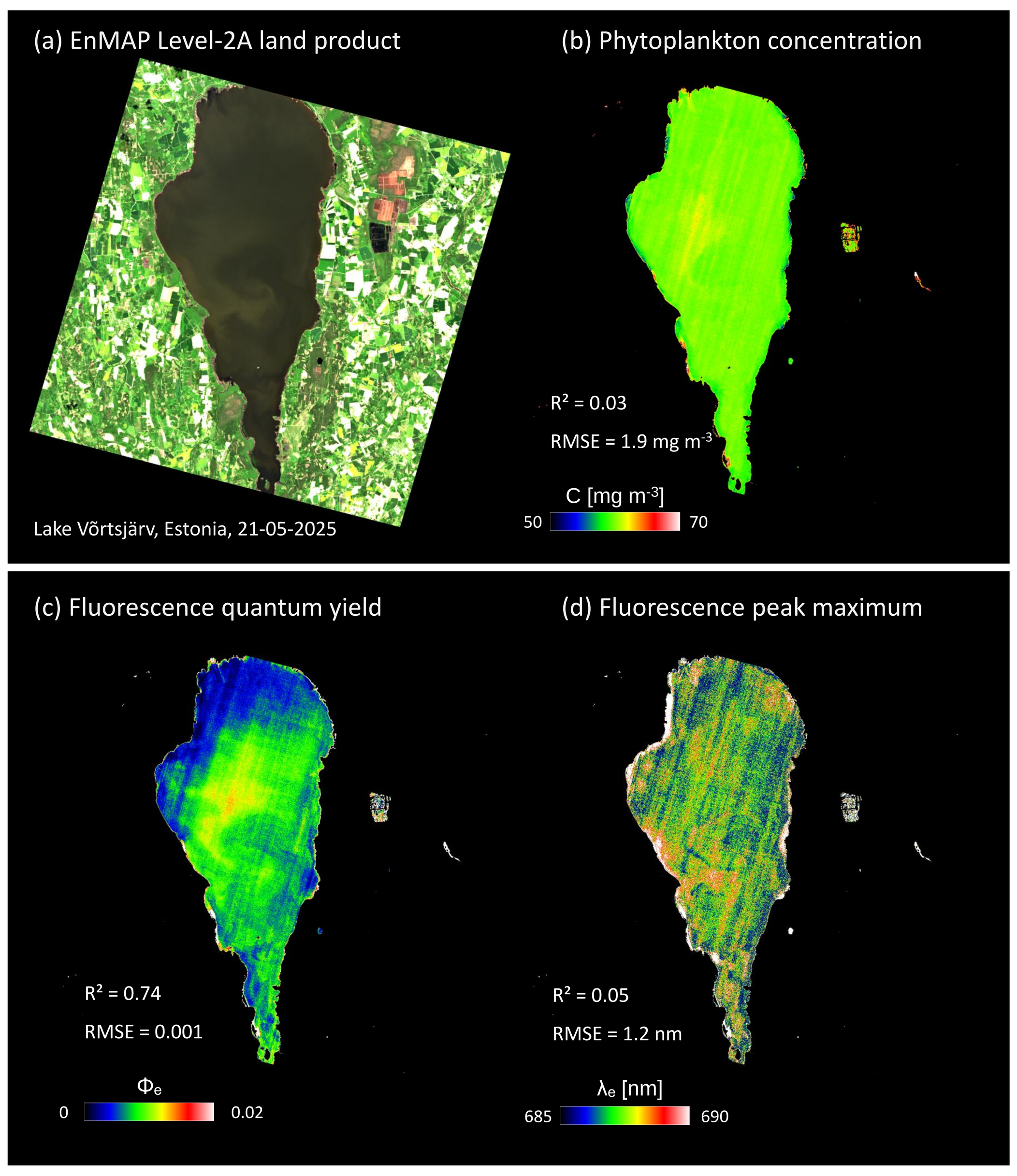

Fig. 3: Results for Lake Võrtsjärv, Estonia. (a) EnMAP image. (b) Phytoplankton concentration map derived in a first step ignoring fluorescence. As variability is too low to reliably quantify concentration differences (R^2 = 0.03), C was kept constant at the average of 60 mg m^{-3} in the second step deriving Φ_e and λ_e. (c) Quantum yield map with Φ_e ranging from 0.003 to 0.011. (d) Peak maximum map with a λ_e average of 687.2 nm; the low variability makes the derived distribution unreliable (R^2 = 0.05).